IL-8 as Antibody Therapeutic Target in Inflammatory Diseases: Reduction of Clinical Activity in Palmoplantar Pustulosis[1]

Lone Skov,* Frank J. Beurskens,† Claus O. C. Zachariae,* Sakari Reitamo,‡ Jessica Teeling,[2†] David Satijn,† Kim M. Knudsen,¶ Elmieke P. J. Boot,† Debra Hudson,§ Ole Baadsgaard,¶ Paul W. H. I. Parren,[3†] and Jan G. J. van de Winkel†‖

IL-8 is a chemokine that has been implicated in a number of inflammatory diseases involving neutrophil activation. HuMab 10F8 is a novel fully human mAb against IL-8, which binds a discontinuous epitope on IL-8 overlapping the receptor binding site, and which effectively neutralizes IL-8-dependent human neutrophil activation and migration. We investigated whether interference in the cytokine network by HuMab 10F8 might benefit patients suffering from palmoplantar pustulosis, a chronic inflammatory skin disease. Treatment of patients with HuMab 10F8 was well tolerated and significantly reduced clinical disease activity at all five endpoints, which included a ≥50% reduction in the formation of fresh pustules. IL-8 neutralization was monitored at the site of inflammation by assessing exudates of palmoplantar pustulosis lesions. HuMab 10F8 sequestered IL-8 in situ, as observed by rapid dose-dependent decreases of IL-8 concentrations immediately following Ab infusion. These data demonstrate a critical role for IL-8 in the pathophysiology of palmoplantar pustulosis. HuMab 10F8 is capable of interrupting IL-8 activity in vivo and represents a candidate for treatment of inflammatory diseases and other pathological conditions associated with IL-8 overproduction. ***The Journal of Immunology,*** **2008, 181: 669–679.**

Chronic inflammatory conditions often result from aberrant production of proinflammatory factors such as chemokines. One chemokine implicated in chronic inflammation is IL-8 (1). IL-8 is a member of the CXC chemokine family and was initially identified as a neutrophil chemotactic and activating factor (2–6). Since then, a variety of other proinflammatory activities have been attributed to IL-8 (7), including immune cell activation (8) and promotion of angiogenesis (9, 10). IL-8 can be produced by a variety of cell types involved in inflammation, including monocytes and endothelial cells. Activation of cells occurs after binding to the IL-8 receptors, CXCR1 and CXCR2, expressed on neutrophils, monocytes, endothelial cells, astrocytes, and microglia (8, 11, 12).

Aberrant IL-8 production can lead to chronic inflammatory conditions, as suggested for inflammatory diseases such as rheumatoid arthritis (13–15), inflammatory bowel disease (16), psoriasis (17, 18), and palmoplantar pustulosis (PPP)[4] (19, 20). Accumulation of activated neutrophils in lesional areas and elevated IL-8 production is observed in all these diseases. In several animal models of acute inflammatory disease, neutralizing Abs against IL-8 inhibit neutrophil function and resolve inflammation (21–24). Hence, abrogation of IL-8 activity represents a candidate therapeutic strategy for chronic inflammatory diseases. We aimed to establish an in vivo proof of this concept in PPP, which is a rare chronic inflammation of the skin that is clinically characterized by recurrent eruptions of sterile pustules on the palms and/or soles. PPP is more often observed in females than in males, the onset is between 20 and 60 years of age, and the disease is positively correlated with smoking and diseases of the thyroid gland. Novel therapeutic strategies for PPP are needed, because this disease is very resistant to current treatments (25, 26).

We generated a fully human anti-IL-8 mAb, characterized its IL-8 inhibitory capacity and binding epitope, and performed a single dose escalation study followed by a 4-wk multiple dose extension in patients with PPP. The marked reduction in disease activity following treatment as reported herein demonstrates a central role for IL-8 in the pathogenesis of PPP and highlights the potential of HuMab 10F8 for immunotherapy of pathologic conditions relating to IL-8 overexpression.

Materials and Methods

Generation of human Abs against IL-8

Human Ig transgenic mice, strain HCo7 (Medarex), were immunized by i.p. injection of recombinant human IL-8 (rhIL-8; Biosite Diagnostics) dispersed in complete or IFA (Sigma-Aldrich). Mice developing human anti-IL-8 Ab, as detected in serum by ELISA, were boosted by i.v. injection

*Department of Dermatology, Copenhagen University Hospital Gentofte, Hellerup, Denmark; †Genmab BV, Utrecht, The Netherlands; ‡Department of Dermatology, University of Helsinki, Hospital for Skin and Allergic Diseases, Helsinki, Finland; §Medarex, Milpitas, CA 95035; ¶Genmab A/S, Copenhagen, Denmark; and ‖Immunotherapy Laboratory, Department of Immunology, University Medical Center, Utrecht, The Netherlands

Received for publication December 14, 2007. Accepted for publication April 16, 2008.

The costs of publication of this article were defrayed in part by the payment of page charges. This article must therefore be hereby marked *advertisement* in accordance with 18 U.S.C. Section 1734 solely to indicate this fact.

[1] This work was supported by Genmab A/S and Medarex.

[2] Current address: Central Nervous System Inflammation Group, University of Southampton, Southampton, U.K.

[3] Address correspondence and reprint requests to Dr. Paul W. H. I. Parren, Genmab BV, Yalelaan 60, 3584 CM, Utrecht, The Netherlands. E-mail address: P.Parren@genmab.com

[4] Abbreviations used in this paper: PPP, palmoplantar pustulosis; rhIL-8, recombinant human IL-8; HAHA, human anti-human Ab; MIG, monokine induced by IFN-γ.

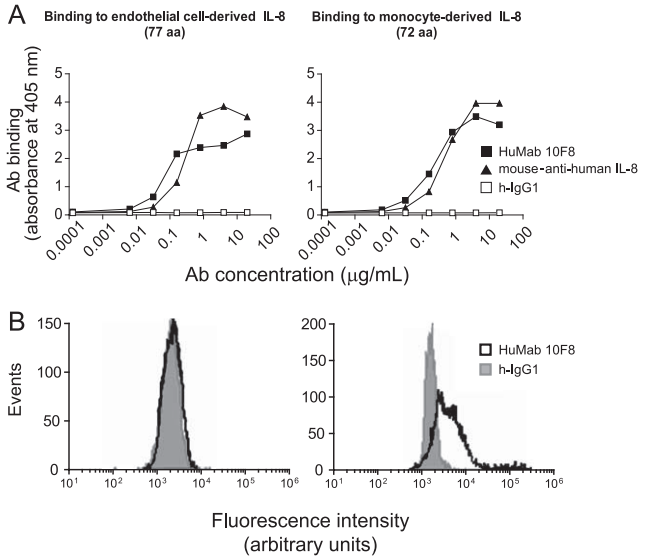

FIGURE 1. Binding characteristics of HuMab 10F8. Binding of HuMab 10F8 to human IL-8 was determined by ELISA (*A*) and flow cytometry (*B*). *A*, ELISA plates were coated with endothelial cell-derived rhIL-8 (*left*) or monocyte-derived rhIL-8 (*right*), and incubated with HuMab 10F8 (■), mouse-anti-human IL-8 (▲), or with control human IgG1 (□). Binding of primary Abs was detected by HRP-conjugated anti-human IgG or anti-mouse IgG and addition of ABTS substrate, and absorbance was measured at 405 nm. Results from one representative experiment out of three are shown. *B*, Peripheral whole blood from healthy human subjects was incubated with LPS to induce IL-8 production. Intracellular IL-8 was detected by staining of permeabilized cells with Alexa Fluor 488-conjugated HuMab 10F8 (open histograms) or isotype control (filled histograms). Histograms of Alexa Fluor 488 fluorescence intensity are shown for nonstimulated cells (*left*) and for cells stimulated for 2 h with LPS (*right*). Results from one representative experiment out of three are shown.

with rhIL-8. Experiments were reviewed and approved by the local Animal Ethics Committee. Spleen and lymph node cells were fused with SP2/0 cells (27), and specific hybridoma clones were selected and subjected to limiting dilution at least twice to ensure monoclonality. Three human mAbs were obtained that were specific for human IL-8 and were of the IgG1κ subclass. Of this panel, HuMab 10F8 (HuMax-Inflam; HuMax-IL8) was selected for further evaluation.

IL-8 affinity determination

RhIL-8 was immobilized on a CM-5 sensor chip (Biacore) via amine chemistry. HuMab 10F8 whole IgG or Fab fragments (prepared using the ImmunoPure Fab preparation kit, Pierce Biotechnology) were injected, and binding was detected using surface plasmon resonance on a Biacore 3000 (Biacore).

IL-8 binding by ELISA

ELISA plates were coated with endothelial cell-derived rhIL-8_{77aa}, monocyte-derived rhIL-8_{72aa} Gro-α, Gro-β, or IP-10 (Strathmann Biotech). Plates were washed with PBS-Tween (PBS supplemented with 0.05% (v/v) Tween 20) and nonspecific binding was blocked with PBS-Tween supplemented with 2% (v/v) chicken serum (Sigma-Aldrich). Plates were then incubated with HuMab 10F8, mouse-anti-human IL-8 (MAK-IL-8, Strathmann Biotech), or with control human IgG1 (Genmab). Bound primary Ab was detected by HRP-conjugated rabbit-anti-human IgG F(ab′)2 (DakoCytomation) or rabbit-anti-mouse IgG F(ab′)2 (Jackson ImmunoResearch Laboratories) and addition of ABTS substrate. Absorbance was measured at 405 nm.

Binding to intracellular IL-8 in human PBMC by flow cytometry

Heparinized peripheral whole blood from healthy volunteers was diluted 1/1 in culture medium (IMDM supplemented with 100 IU/ml penicillin, 100 μg/ml streptomycin (all from Invitrogen), and 1% CCS (HyClone)). Diluted blood was stimulated with 100 μg/ml LPS (*E. coli* serotype 026: B6, Sigma-Aldrich) for 2 h at 37°C, together with GolgiStop (monensin, Cytofix/Cytoperm Kit, BD Pharmingen) to accumulate IL-8 intracellularly. Cells were lysed in BD lysing solution (BD Pharmingen). Cells were washed by centrifugation and resuspended in Cytofix/Cytoperm solution (BD Pharmingen). Intracellular IL-8 was detected by staining with Alexa Fluor 488-conjugated HuMab 10F8 in Perm/Wash buffer (BD Pharmingen), and HuMab-KLH-Alexa Fluor 488 (Genmab) was used as isotype control. Cell-associated fluorescence was analyzed using a FACSCanto II and FACSDiva software (BD Biosciences).

Determination of IL-8 binding epitope

Pepscan Chemically Linked Peptides on Scaffolds technology (28, 29) was used to determine the IL-8 epitope to which HuMab 10F8 is directed. Approximately 2000 different peptides were designed based on the amino acid sequence of IL-8_{77aa} (endothelial cell-derived) and used in Pepscan screening either as linear peptides or linked to scaffolds to yield 30-mer single-, double-, or triple-looped or sheetlike peptides. Binding of HuMab 10F8 (1 μg/ml) to the resulting peptides was determined using anti-human-peroxidase (1/1000) as detection agent.

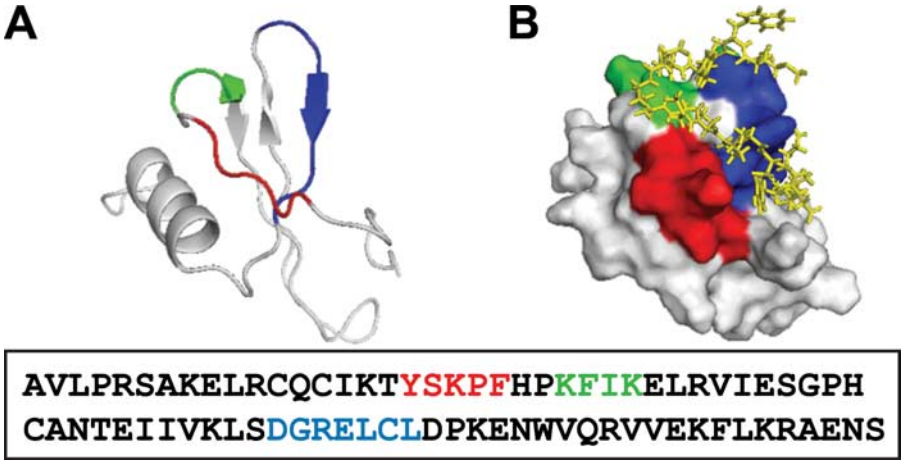

FIGURE 2. Schematic representation of the HuMab 10F8 binding epitope on human IL-8. The binding epitope of HuMab 10F8 was determined using Pepscan Chemically Linked Peptides on Scaffolds technology. *A*, The three identified binding regions are depicted in red, green, and blue on a cartoon structure representation of human IL-8. *B*, The surface structure representation of human IL-8 interacting with residues P21–P29 of CXCR1 (shown as licorice structure representation in yellow) as previously described (33) was adapted to show that these CXCR1 residues occupy a hydrophobic groove between the N-terminal loop and the β3 strand of hIL-8 corresponding to the HuMab-10F8 binding epitope. *Bottom*, Amino acid sequence of human IL-8 with HuMab 10F8 binding regions indicated in red, green, and blue.

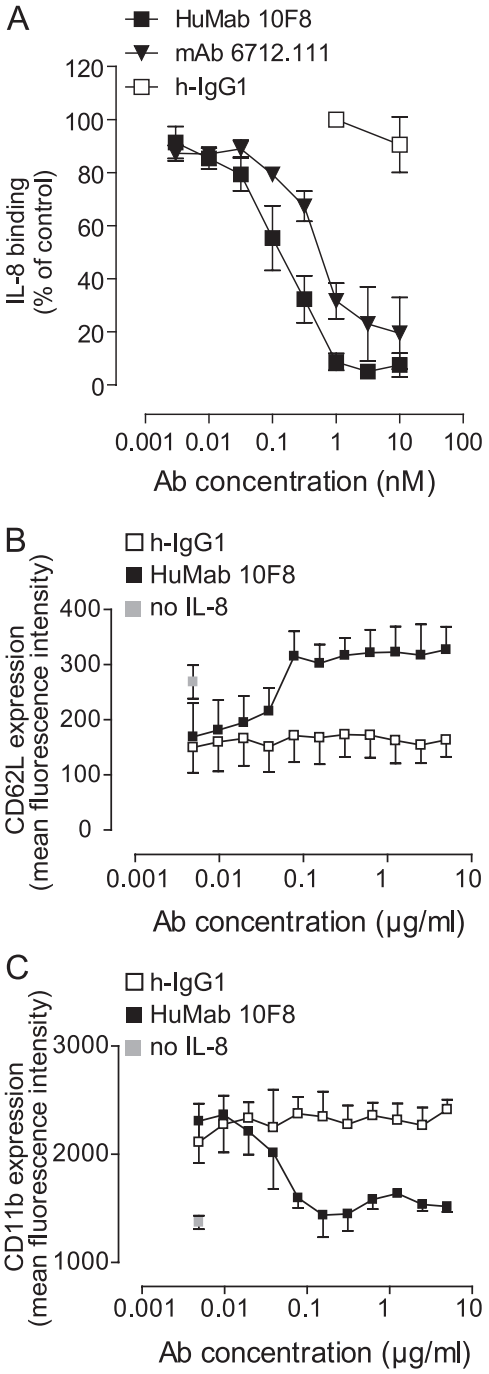

FIGURE 3. Effect of HuMab 10F8 on [^{125}I]IL-8 binding to neutrophils and IL-8-mediated neutrophil activation. *A*, To study inhibition of IL-8 binding to cells, human neutrophils were incubated with [^{125}I]IL-8 and a concentration range of HuMab 10F8 (■), the positive control mouse-anti-human IL-8 mAb 6712.111 (▲), or human IgG1 as negative control (□). Unbound [^{125}I]IL-8 was captured on filters and analyzed using a Wallac gamma counter. Results represent means ± SEM of three independent experiments. IC_{50} values were determined using a nonlinear regression (allowing variable slopes) of the separate experiments: 0.3 ± 0.2 nM for 10F8, 1.6 ± 1.1 nM for the reference mAb. *B* and *C*, Peripheral whole blood was stimulated with rhIL-8 in the presence of HuMab 10F8 (■) or control human IgG1 (□), or in the absence of both Ab and rhIL-8 (▩). Expression of CD62L (*B*) and CD11b (*C*) was assessed by flow cytometry. Data represent the mean fluorescence intensity (means ± SEM of three experiments).

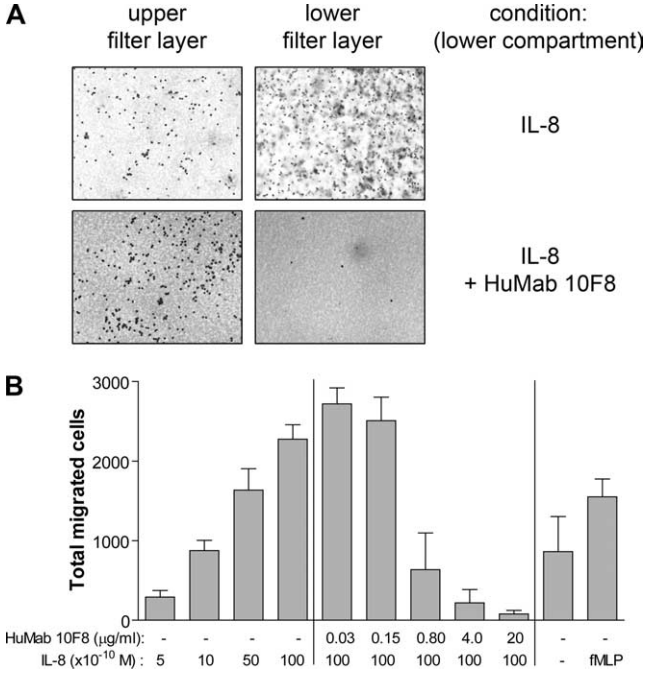

FIGURE 4. Inhibition of IL-8-mediated human neutrophil chemotaxis by HuMab 10F8. Neutrophil chemotaxis was studied using a Boyden chamber system, with neutrophils in the upper compartment and rhIL-8 in the presence or absence of HuMab 10F8 in the lower compartment. fMLP (10^{-8} M) was used as positive control. Neutrophil migration was quantified after 1 h incubation at 37°C. *A*, Representative images are shown of the upper and lower layer of the filter between compartments, with IL-8 (10^{-8} M) in the lower compartment in the absence or presence HuMab 10F8 (4 µg/ml). *B*, Results are shown as the total number of migrated cells (means ± SD of triplicates).

Inhibition of IL-8 binding to human neutrophils

Neutrophils were enriched from heparinized peripheral blood from healthy volunteers by Ficoll density gradient centrifugation (room temperature, 400 × *g*, 30 min) and erythrocytes were removed by hypotonic shock. Enriched neutrophils were resuspended in PBS containing 0.1% BSA and 0.02% sodium azide (PBA buffer). The IL-8 inhibition of binding assay was performed as previously described (30) with 4×10^5 neutrophils per well using [^{125}I]rhIL-8 (Amersham Life Sciences) and HuMab 10F8, mouse-anti-human IL-8 mAb (clone 6712.111, R&D Systems), or human IgG1 (Medarex). IC_{50} values were determined using a nonlinear regression (allowing variable slopes) of the separate experiments (mean IC_{50} ± SEM).

Neutrophil activation marker expression

Heparinized peripheral blood from healthy volunteers was diluted 1/5 (v/v) in culture medium and incubated with serial dilutions of HuMab 10F8 in the absence or presence of 25 ng/ml rhIL-8 (PeproTech) (37°C, 2 h). Cells were then incubated with PE-conjugated mouse-anti-human CD11b or FITC-conjugated mouse-anti-human CD62L (BD Pharmingen) (4°C, 30 min). Erythrocytes were lysed with FACS lysing solution (BD Pharmingen), and cell-associated fluorescence was analyzed by flow cytometry.

Neutrophil chemotaxis assay

Neutrophil chemotaxis was studied using the Boyden chamber system. Neutrophils enriched from heparinized peripheral blood from normal volunteers (4×10^5 cells) were transferred to the upper compartment of a Boyden chamber. RhIL-8 (PeproTech) and HuMab 10F8 were added to the lower compartment, chambers were incubated for 1 h at 37°C, and cell migration was quantified by microscopic inspection of the filter (pore width 8 µm, thickness 150 µm; Sartorius). The synthetic neutrophil chemoattractant fMLP (Sigma-Aldrich) was used as a positive control. At 15 intervals of 10 µm, the total cell number and the total distance migrated were scored in the Z-direction of the filter. Cells in layer 1 were excluded for calculation of the total number of migrated cells, the total migrated distance, and the mean migration per cell. Alternatively, neutrophil chemotaxis was studied using a transwell sytem. RhIL-8 and HuMab 10F8, mouse-anti-human IL-8 mAb (clone 6712.111, R&D Systems), and control human IgG1 (Medarex) were added to one compartment on a transwell plate. Neutrophils were transferred to the other compartment. Plates were

Table I. *Presence of IL-8 and other chemokines in washing fluids from PPP patients*

Cytokine/chemokine[a]	Controls[b] Concentration (ng/ml) [No. Patients Evaluated][c]	PPP Patients[b] Concentration (ng/ml) [No. Patients Evaluated][c]	PPP Patients[b] Incidence	Eczema Patients[b] Concentration (ng/ml) [No. Patients Evaluated][c]	Eczema Patients[b] Incidence
IL-6	0.4 ± 0.2 [5]	38.9 ± 49.4 [6]	6/6	33.2 ± 37.6 [6]	6/6
IL-8	47.8 ± 31.3 [6]	7,382.6 ± 3,695.5 [6]	6/6	3,025.7 ± 2,834.0 [6]	6/6
MCP-1	0.0 ± 0.0 [5]	1.2 ± 2.6 [6]	5/6	2.3 ± 4.0 [6]	6/6
MIG	566.5 ± 381.3 [6]	7,646.2 ± 9,752.7 [6]	2/6	15,555.6 ± 15,392.1 [6]	4/6
IL-12p40	35.0 ± 24.4 [5]	398.5 ± 698.8 [6]	2/6	62.0 ± 35.3 [6]	0/6

[a] Washing fluids from PPP patients, eczema patients, and healthy controls were analyzed by protein array for the presence of cytokines/chemokines. Data are shown for cytokines/chemokines that were elevated in PPP fluid (mean log concentration$_{PPP}$ ≥ mean log concentration$_{controls}$ + 2× SD log concentration$_{controls}$). For eotaxin, G-CSF, GM-CSF, IFN-γ, IL-10, IL-12p70, IL-13, IL-15, IL-1α, IL-1β, IL-2, IL-3, IL-4, IL-5, IL-7, IP-10, MCP-3, TGF-β, TNF-α, TNF-β, TRAIL, and sCD95, the relative expression was not elevated in any condition.

[b] Results are shown as mean cytokine/chemokine concentrations ± SD (ng/ml), and as incidence of increase (number of patients showing increased cytokine/chemokine levels). Concentrations were considered increased when log concentration$_{PPP/eczema}$ ≥ mean log concentration$_{controls}$ + 2× SD log concentration$_{controls}$.

[c] Only samples in which cytokine/chemokines were above the level of quantification have been included in the table.

incubated for 2 h at 37°C, and cell migration was quantified by microscopic inspection (data not shown).

Evaluation of IL-8 and other cytokines and chemokines in PPP washing fluids

Washing fluid of six PPP patients was obtained as described previously (17) from the most severely afflicted hand or foot based on pustule counts (i.e., the number of fresh pustules on the plantar and palmar side of hand/foot). As a control, washing fluid was obtained from six patients with hand eczema and from six healthy controls. Briefly, the hand or foot was inserted into a plastic bag with 2 ml of saline for 30 min, washing fluid was aspirated, the volume was determined, and the fluid was stored at −20°C until analysis. Washing fluid was examined for the presence of eotaxin, G-CSF, GM-CSF, IFN-γ, IL-1α, IL-1β, IL-2, IL-3, IL-4, IL-5, IL-6, IL-7, IL-8, IL-10, IL-12p40, IL-12p40/p70, IL-12p70, IL-13, IL-15, IP-10, MCP-1, MCP-3, monokine induced by IFN-γ (MIG), sCD23, sCD95, sICAM-1, TGF-β, TNF-α, TNF-β, and TRAIL using the human cytokine Protein Profiling Biochip technology (Zyomyx). IL-8, Gro-α, C5a, and ENA-78 concentrations were also determined by ELISA using commercially available ELISA kits (IL-8 PeliKine Compact (Sanquin); Quantikine human IL-8 kit, Quantikine human Gro-α kit, and Quantikine ENA-78 kit (R&D Systems); and C5a kit (OptEIA via BD Pharmingen)). Normal human serum was used as a negative control.

Clinical trial: study design and population

An open-label multicenter study was performed with a single dose dose-escalation setup followed by a 4-wk multiple dose extension. The clinical study was performed at three university hospitals in Denmark (Copenhagen University Hospital, Gentofte; County Hospital, Roskilde; Aarhus University Hospital, Aarhus), one in Finland (Hospital for Skin and Allergic Diseases, Helsinki), and one private dermatology practice in Denmark (Aalborg Hudklinik, Aalborg). The study was conducted according to the Declaration of Helsinki, and the study protocol was identical for all study sites and was reviewed and approved by the human research ethics committees for each of the five study sites. All patients gave written informed consent before inclusion in the study. The study was performed as a single dose dose-escalation including single dose levels of 0.15, 0.5, 1, 2, 4, and 8 mg/kg. The next dose level was initiated after safety evaluation of the previous dose level, including dose-limiting toxicity for 2 wk. Four weeks after the single dose, patients entered the repeated-dose extension comprising four administrations once per week, including dose levels of 0.15, 0.5, 1, 2, and 4 mg/kg. Patients receiving 8 mg/kg as a single dose received 4 mg/kg as a repeating dose. All other patients continued repeat dosing of the initial single dose level. Patients were followed for an additional 4 wk. HuMab 10F8 was administered by i.v. infusion during 60 min in one arm.

Of the 32 PPP patients planned for inclusion, 31 were enrolled from April 2003 until May 2004. All patients, recruited in Denmark and Finland, 18 years or older, were clinically diagnosed with palmoplantar pustulosis of at least 6 mo duration by a board-certified dermatologist (patients with psoriasis were excluded) and were suffering from active disease (defined as having at least a total of 20 fresh pustules on the soles or palms at screening). None of the patients had received systemic therapies for PPP or UV therapies within 4 wk before the start of the study or any topical therapies or devices (e.g., hydrocolloid occlusion) within 2 wk before the start of the study. Use of nonsteroid antiinflammatory drugs (NSAID) was allowed, but patients receiving systemic immunosuppressive or antiinflammatory therapies (other than NSAID) or having received prior treatment with anti-IL-8 mAb were excluded. Patients were excluded from the study for any of

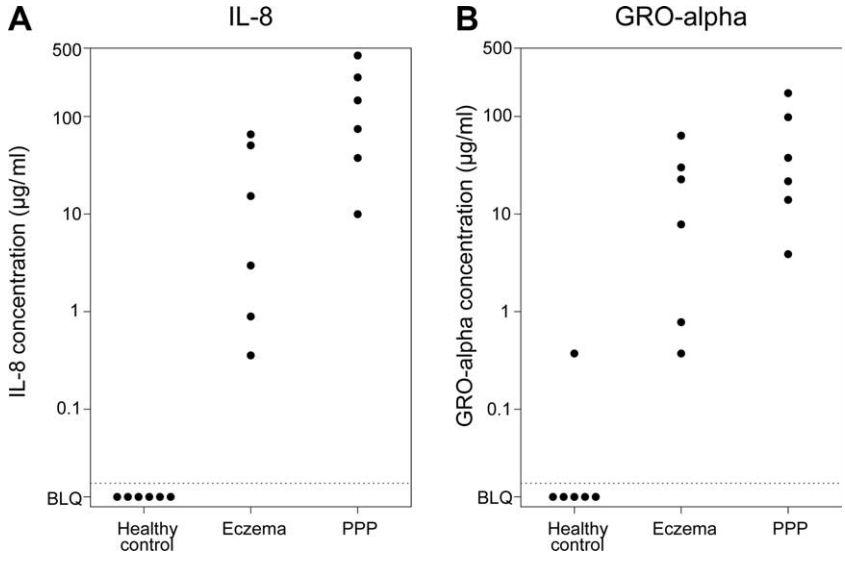

FIGURE 5. Elevated levels of IL-8 and Gro-α in PPP washing fluid. PPP, eczema, and control washing fluids were analyzed for the level of IL-8 (*A*) and Gro-α (*B*) by sandwich ELISA. Results of individual measurements are shown as the concentration of the respective chemokines per milliliter of fluid in $n = 6$ subjects/group. BLQ, Below level of quantification.

Table II. *Patient baseline characteristics*

Patient Characteristics	HuMab 10F8 Dose Group (No. of Patients)					
	0.15 mg/kg ($n = 4$)	0.5 mg/kg ($n = 4$)	1 mg/kg ($n = 4$)	2 mg/kg ($n = 4$)	4 mg/kg ($n = 8$)	8/4 mg/kg ($n = 7$)
Age (years), median (range)	67 (57–68)	57 (44–60)	64 (54–70)	50 (42–62)	50 (42–62)	54 (41–71)
Male/female	1/3	2/2	0/4	0/4	2/6	1/6
Weight (kg), median (range)	68 (62–92)	75 (70–102)	60 (52–73)	63 (60–79)	71 (52–90)	65 (45–94)
Thyroid stimulating hormone (μU/ml), median (range)	1.4 (0.6–3.5)	1.7 (1.2–2.4)	1.3 (0.6–2.3)	1.9 (0.6–2.7)	1.8 (0.9–3)	1.5 (0.6–4.2)
Duration of PPP (years), median (range)	8 (2.3–16.5)	6 (2.2–14.5)	14 (0.5–18.7)	7 (4.5–14.8)	10 (1.1–27)	5 (0.5–43.1)
Disease activity (no. of pustules),[a] median (range)	48 (26–144)	26 (7–71)	63 (41–72)	21 (11–24)	29 (5–90)	46 (13–235)

[a] Total number of fresh pustules at baseline (week 0).

the following reasons: immunodeficiency, past or current malignancy, acute or chronic infection, and clinically significant cardiac or cerebrovascular disease. Pregnant or breast-feeding women were not enrolled in the study, and women with childbearing potential were to use a contraceptive.

Response criteria and safety

The efficacy endpoints were: 1) number of fresh pustules (white to yellow pustules of at least 1 mm); 2) clinical response (≥50% reduction in the number of fresh pustules compared with baseline (i.e., week 0) for the single dose period, or to week 4 for the multiple dose period); 3) PPP composite severity index taking into account extent of involvement (25, 26) (i.e., area of involved skin, rated from 0 to 100% of the entire skin surface of the region), severity of erythema, infiltration, and scaling (rated from 0 to 3); 4) Physician's Global Assessment (visual analog scale); and 5) Patient's Symptom Assessment (visual analog scale).

To assess the efficacy of HuMab 10F8 in situ, the IL-8 concentration in hand or foot washing fluid was determined by ELISA. Washing fluid was obtained at baseline and weeks 1, 4, and 8 from the most severely afflicted hand or foot as described above; in case of hand washing fluid, the hand at the noninfused arm was used. On the treatment days (baseline and week 4), washing fluid was obtained during infusion of HuMab 10F8. Patients were also assessed for dose-limiting toxicity and adverse events in general. At all visits, patients were asked for occurrence of adverse events, and vital signs and ECG were evaluated. Blood was sampled for standard hematology and clinical chemistry at all visits except two. Samples to assess potential development of human anti-human antibodies (HAHA) were collected at baseline and weeks 4 and 10 and analyzed by ELISA. IL-8, Gro-α, C5a, and ENA-78 concentrations in washing fluid were determined by ELISA as described above. Also, the concentration of free HuMab 10F8 in the same washing fluid samples was quantified by ELISA. Briefly, rhIL-8 (0.5 μg/ml in PBS; PeproTech) was coated onto ELISA plates. After washing with PBS-Tween and blocking of nonspecific binding with PBS supplemented with 2% (v/v) chicken serum (Invitrogen), plates were incubated with serial dilutions of PPP samples. HuMab 10F8 was detected using goat-anti-human IgG-HRP (Jackson ImmunoResearch Laboratories) and ABTS substrate. Absorbance was measured at 405 nm. The concentration of free HuMab 10F8 was calculated using a HuMab 10F8 standard curve. All samples for a specific laboratory parameter were assessed by a central laboratory. Note that one patient in the 4 mg/kg group displayed a PK profile indicating erroneous infusion administration or measuring.

Statistical evaluation

The differences in chemokine levels between PPP and eczema samples were analyzed using a t test or a Wilcoxon test for comparisons with healthy control samples. In the analysis of clinical trial data, change from baseline in pustule count was analyzed using a paired t test of log pustule count. A p value <0.05 was considered to be significant. For all data, descriptive statistics were applied.

Results

Generation of a human mAb against human IL-8 and binding characteristics of HuMab 10F8

A fully human mAb against human IL-8 was generated using human Ig transgenic mice (31). Mice were immunized with IL-8, and hybridomas were obtained using somatic cell fusion. HuMab 10F8 was selected for further studies because of its excellent IL-8-binding characteristics and efficient inhibition of IL-8 binding to neutrophils and neutrophil chemotaxis. The binding constant of HuMab 10F8 was determined by surface plasmon resonance in Biacore. The affinity of HuMab 10F8 Fab fragments for rhIL-8 was 372 pM at 37°C (k_a of 1.06×10^5 M^{-1} sec^{-1}, k_d of 3.94×10^{-5} sec^{-1}). When testing HuMab 10F8 whole IgG1, the avidity was 20 pM at 37°C (K_a of 2.75×10^5 M/sec; K_d of 0.54×10^{-5}/sec). The binding of HuMab 10F8 to rhIL-8_{72aa} (72 aa form of IL-8 as derived from monocytes) and rhIL-8_{77aa} (77 aa form of IL-8 as derived from endothelial cells) and the homologous chemokines rhGro-α, rhGro-β, and rhIP-10 was assessed by ELISA. HuMab 10F8 bound to plate-bound, monocyte-derived, and endothelial cell-derived IL-8 (Fig. 1*A*) and did not cross-react with Gro-α, Gro-β, or IP-10 (data not shown). Binding of HuMab 10F8 to native human IL-8 was confirmed by staining of intracellular IL-8 in LPS-activated human peripheral blood cells and analysis by flow cytometry (Fig. 1*B*) and immunocytochemistry (data not shown).

Binding epitope of HuMab 10F8

The HuMab 10F8 epitope on IL-8 was determined via Pepscan Chemically Linked Peptides on Scaffolds technology (28, 29). Approximately 2000 different peptides were designed based on the IL-8 amino acid sequence (77 aa form) and used in Pepscan screening either as linear peptides (15-mers) or linked to scaffolds to yield 30-mer single-, double-, or triple-looped or sheetlike peptides. Three different binding regions were identified: YSKPF (IL-8_{18-22}), KFIK

FIGURE 6. Effective treatment of PPP with HuMab 10F8. Improvement in PPP from baseline (*A*) to 1 wk after the first dose (*B*), 1 wk after multiple doses (*C*), and 3 wk after the multiple dose phase (*D*) in a patient treated with HuMab 10F8, 8 mg/kg as single dose, followed by 4 mg/kg as repeating dose.

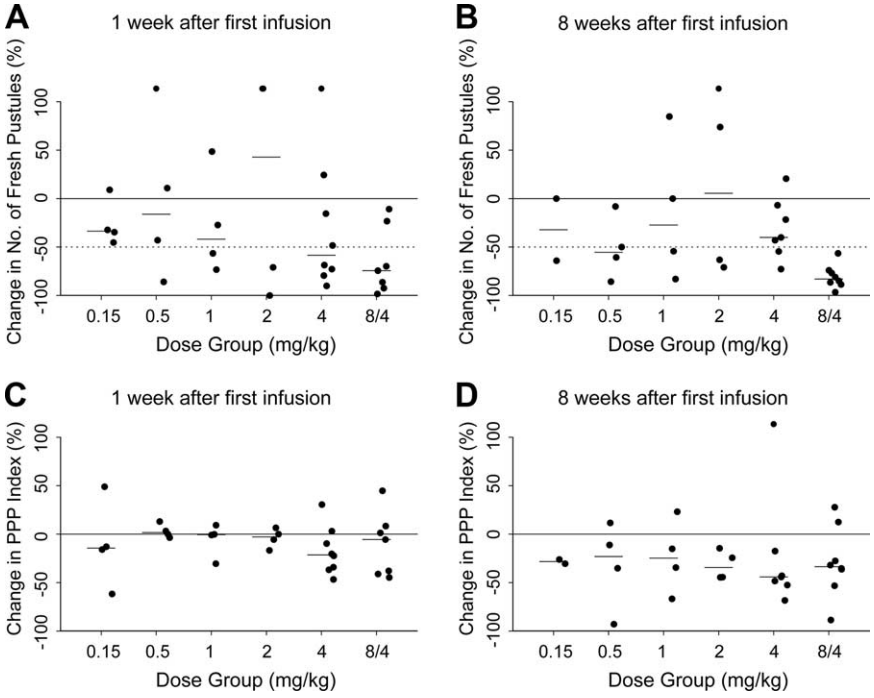

FIGURE 7. Change in number of fresh pustules and PPP composite severity index during treatment with HuMab 10F8. The number of fresh pustules (white to yellow pustules of at least 1 mm seen from the plantar or palmar view) and the PPP composite severity index (extent of involvement and severity of erythema, infiltration, and scaling) was measured at each visit. The change in numbers of fresh pustules following single dose (week 0 to week 1, *A*) and for the whole treatment period (week 0 to week 8, *B*) for each dose group is shown. The changes in PPP composite severity index following single dose (week 0 to week 1, *C*) and for the whole treatment period (week 0 to week 8, *D*) are shown. The median values in each group are indicated by a horizontal line.

($IL\text{-}8_{25-28}$), and DGRELCL ($IL\text{-}8_{50-56}$). The region YSKPF with KP as its core region was recognized in both linear and looped topology, and it was found to represent the dominant binding region. Combining YSKPF with DGRELCL in a double-looped topology gave the best binding activity, indicating that DGRELCL contributed to binding and is part of the HuMab 10F8 epitope. The region KFIKELRV was the third region found to have binding activity, independent of the other two binding regions. Taken together, these data indicated that HuMab 10F8 recognizes a discontinuous epitope on human IL-8 comprising all of the three identified regions (Fig. 2, *A* and *bottom panel*). The identified HuMab 10F8 epitope overlaps with the binding site of CXCR1 (Fig. 2*B*).

Inhibition of IL-8 bioactivity by HuMab 10F8

The ability of HuMab 10F8 to inhibit IL-8 activity was first assessed in vitro. To analyze inhibition of IL-8 receptor binding, neutrophils were enriched from human peripheral blood and incubated with radiolabeled rhIL-8 in the presence of HuMab 10F8. HuMab 10F8 dose-dependently inhibited binding of IL-8 to human neutrophils (Fig. 3*A*) with an IC_{50} at 0.3 nM (compared with 1.6 nM for a positive control mAb).

To study whether HuMab 10F8 inhibited IL-8-induced neutrophil activation, we incubated whole blood cells with HuMab 10F8 and determined CD11b up-regulation and CD62L down-regulation in the presence/absence of rhIL-8. HuMab 10F8 potently and dose-dependently inhibited both the induction of CD11b expression by IL-8 on neutrophils (Fig. 3*C*), as well as the shedding of CD62L (Fig. 3*B*) from these cells.

We studied the effect of HuMab 10F8 on neutrophil chemotaxis, because the recruitment of neutrophils to sites of inflammation represents an important IL-8 function. Neutrophil migration was assessed using a Boyden chamber system, with neutrophils in the upper compartment and rhIL-8 alone or with HuMab 10F8 in the lower compartment. Neutrophils readily migrated toward IL-8,

Table III. *Adverse events in PPP patients treated with HuMab 10F8*

	Dose Group													
	0.15 mg/kg		0.5 mg/kg		1.0 mg/kg		2.0 mg/kg		4.0 mg/kg		8/4 mg/kg		Total	
	n[a]	E[b]	*n*	E	*n*	E	*n*	E	*n*	E	*n*	E	*n*	E
Patients	4		4		4		4		8		7		31	
Serious adverse events														
Acute myocardial infection	1	1											1	1
Syncope									1	1			1	1
All nonserious adverse events	2	7	3	9	3	12	4	14	7	24	6	19	25	85
Nonserious adverse events in >2 patients[c]														
Headache			1	1	1	1	2	2	1	1	2	3	7	8
Nasopharyngitis			1	1					2	3	2	3	5	7
Nausea			1	1			1	1	1	1	2	2	5	5
Fatigue			1	1			1	1			2	2	4	4
Hematuria							2	2	1	1	1	1	4	4

[a] Number of patients.
[b] Number of events.
[c] Nonserious adverse events occurring in two patients: malaise, edema peripheral, rigors, cystitis, urticaria, leukocyturia, hypercholesterolemia; remaining nonserious adverse events occurred only once.

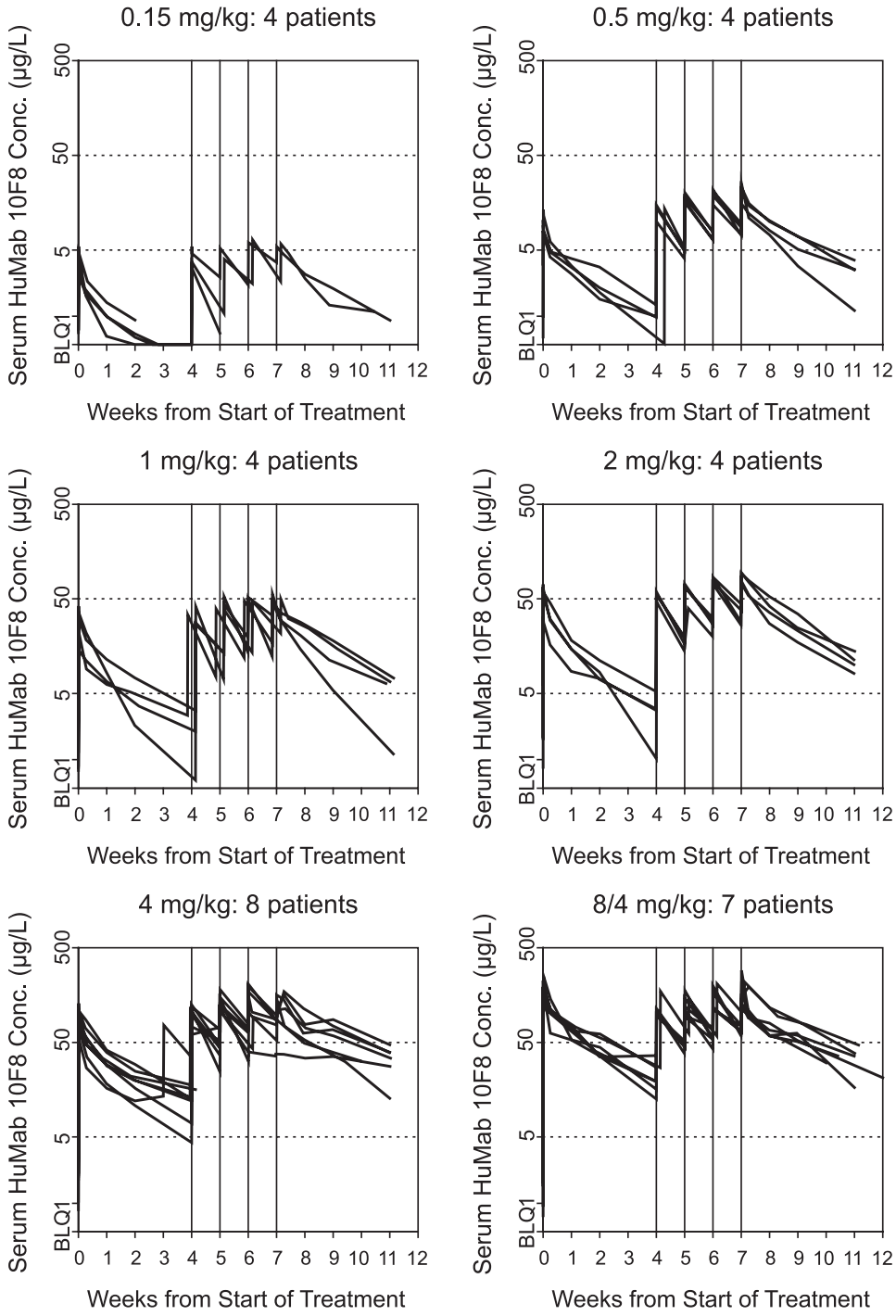

FIGURE 8. HuMab 10F8 plasma concentration profiles by dose group. Samples for measurement of HuMab 10F8 concentration in plasma were collected at all visits except at screening. Samples were drawn before dosing at 0, 4, 5, 6, and 7 wk (vertical reference lines). Concentration profiles from each patient are shown across time in each dose group.

which was inhibited in a dose-dependent manner when HuMab 10F8 was present in the lower compartment (Fig. 4). The values for mean migration per cell were 132.7 ± 7.0 μm in the presence of 10^{-8} M IL-8 alone, which was decreased to 132.3 ± 1.2, 128.7 ± 4.0, 71.3 ± 23.5, 56.0 ± 43.7, and 57.0 ± 41.6 μm in the presence of 0.03, 0.15, 0.8, 4, or 20 μg/ml HuMab 10F8. These results were confirmed in a trans-well system (data not shown).

Abundance of IL-8 in PPP washing fluids

PPP represents a chronic inflammatory skin disease characterized by intraepidermal accumulation of neutrophils. The presence of IL-8 in PPP lesional skin biopsies (19, 20) suggested that IL-8 plays a role in PPP pathophysiology. To address the role of IL-8 in relationship to other proinflammatory factors, we measured the levels of IL-8 and other cytokines/chemokines in exudates of PPP lesions. Exudates from PPP patients were obtained as washing fluid by incubating the most severely afflicted hand or foot into a plastic bag with 2 ml of saline for 30 min. As a control, washing fluids from patients with hand eczema and healthy controls were taken in a similar manner. Samples were analyzed for the presence of cytokines and chemokines by protein array and ELISA.

Of all inflammatory mediators tested, only a limited number of cytokines/chemokines were found to be elevated in patients' washing fluids. The relative expression of IL-12p40 was specifically elevated in PPP patients (Table I), while sCD23 and sICAM-1 were specifically elevated in eczema patients (data not shown). IL-6, IL-8, MCP-1, and MIG levels were elevated both in PPP and eczema patients (mean log concentration$_{PPP/eczema}$ ≥ mean log

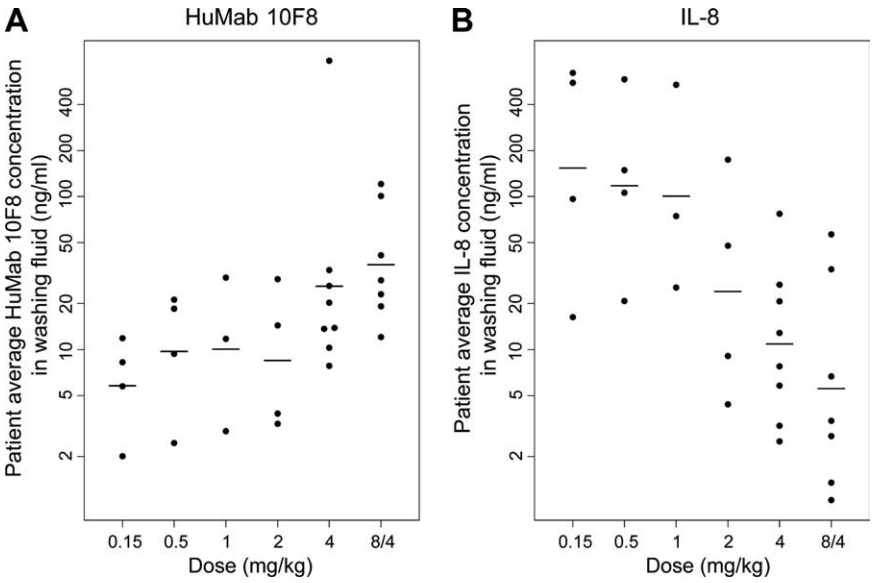

FIGURE 9. Concentration of HuMab 10F8 and IL-8 in PPP washing fluid following HuMab 10F8 treatment. PPP washing fluid of patients treated with HuMab 10F8 was tested for the presence of HuMab 10F8, and IL-8 by sandwich ELISA at 0, 1, 4, and 8 wk. Results shown are the average concentration of HuMab 10F8 (*A*) or IL-8 (*B*) per patient in each dose group (symbols) and the mean within each dose group (horizontal lines).

concentration$_{controls}$ + 2×SD log concentration$_{controls}$; Table I). Absolute IL-8 concentrations were higher in PPP samples compared with samples from eczema patients and healthy controls: IL-8 protein levels were elevated in all PPP patients tested, with a 1.5-log difference in mean concentration from healthy controls (compared with a 0.9-log difference in eczema patients from healthy controls).

The increase of IL-8 in PPP washing fluids was confirmed by ELISA. Both PPP patients and eczema patients showed elevated IL-8 levels compared with healthy controls (Fig. 5*A*). Comparison of washing fluids of PPP and eczema patients demonstrated a much higher IL-8 level in PPP washing fluids (10,000-fold elevation in PPP patients over control, 1,200-fold elevation in eczema patients over control; $p = 0.002$ for PPP from controls, Wilcoxon test, exact two-sided; $p = 0.028$ for PPP from eczema patients, *t* test on logarithmic IL-8 values). The levels of Gro-α (Fig. 5*B*), complement factor C5a, and ENA-78 (data not shown) were also assessed by ELISA. Of these, only Gro-α was found to be significantly elevated in PPP washing fluids compared with eczema patients ($p = 0.175$, *t* test on logarithmic IL-8 values) and to healthy controls ($p = 0.002$, Wilcoxon test, exact two-sided).

Treatment of PPP patients with HuMab 10F8

Thirty-one PPP patients with a median number of fresh pustules of 35 at baseline were included in the study. Patients were allocated to six dose groups: four to 0.15 mg/kg, four to 0.5 mg/kg, four to 1 mg/kg, four to 2 mg/kg, eight to 4 mg/kg, and seven to 8 mg/kg as a single dose. Four weeks after the single dose, patients entered the repeated-dose extension, comprising four administrations once per week of a dose equal to the initial dosing, except the 8 mg/kg initial dosing, which was continued as a 4 mg/kg repeating dose. All patients (25 women and 6 men) were Caucasian with a median age of 57, ranging from 41 to 71 years of age. The median time since diagnosis of PPP was ~8 years, ranging from 6 mo to 43 years. Twenty-six patients were current smokers and the remaining 5 patients were former smokers. Three patients discontinued the study. One refused further participation 14 days after administration of a single dose of 0.15 mg/kg, and one discontinued due to a serious, non-drug-related adverse event 29 days after receiving a single dose of 4 mg/kg. One patient discontinued the study during the multiple dose phase, after two doses of 0.15 mg/kg due to a non-drug-related serious adverse event. Patient baseline characteristics are summarized in Table II.

The numbers of fresh pustules were strongly reduced after both single and multiple dose administrations (Fig. 6). Across all dose groups, there was a reduction of 52.9% from baseline to week 1 ($p = 0.003$), and a reduction of 55.9% from baseline to week 8 ($p = 0.0002$; paired *t* test of log pustule count). The change in numbers of fresh pustules following a single dose (baseline to week 1) and for all data (baseline to week 8) are shown in Fig. 7, *A* and *B*. A clinical response (measured as a decrease of 50% or more in numbers of fresh pustules) was observed after both single and multiple doses. The proportion of patients with a clinical response was between 37% at 4 wk and 61% at 8 wk. In the high-dose group, 7 out of 7 patients showed at least a 50% reduction in numbers of fresh pustules, with 4 patients having a reduction of 75% from baseline to week 8. Following multiple dose administrations, the PPP composite severity index was reduced in 82% (23 out of 28) of patients (Fig. 7*D*). A similar, yet less pronounced tendency was observed after single dose administration in 58% (18 out of 31) of patients (Fig. 7*C*). According to the Physician's Global Assessment, the disease severity was reduced in 71% of the patients after multiple dose administration and in 48% after a single administration (data not shown). According to the Patient's Symptom Assessment, the disease severity was reduced in 82% of the patients after multiple dose administration and in 81% after a single administration (data not shown).

Treatment with HuMab 10F8 was well tolerated

HuMab 10F8 therapy was well tolerated. Twenty-five of the 31 patients (81%) had in total 85 adverse events, which were mostly mild or moderate (Table III). There were two serious adverse events, both considered not related to HuMab 10F8 treatment (acute myocardial infarction and syncope). The adverse events were distributed equally between cohorts; that is, ~80% of patients in each cohort experienced one or more adverse events. Approximately 50% of reported adverse events (45 of 85) were judged attributable to the study drug. The most frequent adverse events were nausea, nasopharyngitis, and headache. There was no increase in frequency of adverse events with increasing dose.

The standard safety panel of serum chemistry and hematology indicated no impact of HuMab 10F8. Samples for HAHA analyses

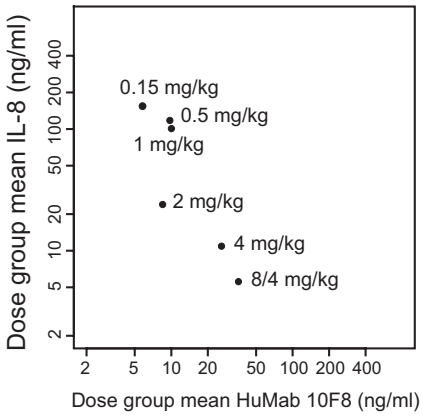

FIGURE 10. Relationship between IL-8 and HuMab 10F8 concentrations following HuMab 10F8 treatment. The mean IL-8 concentrations within each dose group (horizontal lines in Fig. 9*A*) are displayed together with the mean HuMab 10F8 concentrations within each dose group (horizontal lines in Fig. 9*B*).

were collected at weeks 0, 4, and 11. No HAHA development was observed as measured by ELISA, and pharmacokinetics were as expected (see next section).

IL-8 is rapidly sequestered by HuMab 10F8 at sites of inflammation

HuMab 10F8 pharmacokinetics were studied by analyzing plasma concentrations by ELISA. The i.v. infusions of HuMab 10F8 yielded little variation in plasma concentrations between patients within each dose group across time (Fig. 8). The maximum plasma concentrations of HuMab 10F8 linearly increased with increasing dose levels, and plasma clearance rates were dose-independent. Both after single dose administration and after repeated dosing, HuMab 10F8 reached maximum plasma concentrations after ~1 h. Four infusions at intervals of 7 days led to limited accumulation and a maximum plasma concentration that was ~60% higher than following single dose administration.

Washing fluids were obtained during HuMab 10F8 infusion at baseline and week 4, and at follow-up visits at weeks 1 and 8. Samples were analyzed for the presence of HuMab 10F8, IL-8, Gro-α, ENA-78, and C5a by ELISA. HuMab 10F8 was readily detected in washing fluid samples, and the average concentrations were dependent on the doses given to patients (Fig. 9*A*). In line with this, the average IL-8 concentrations in washing fluids decreased with increasing HuMab 10F8 doses (Fig. 9*B*), indicating that HuMab 10F8 is capable of neutralizing IL-8 in situ. For Gro-α, C5a, and ENA-78, no differences were observed between high and low HuMab 10F8 dose groups (data not shown). Moreover, when combining means from Fig. 9*A* with Fig. 9*B*, a monotonic relation with dose level between mean IL-8 concentrations and mean HuMab 10F8 concentrations in washing fluids was observed (Fig. 10).

Discussion

Overproduction of IL-8 has been proposed to significantly contribute to a number of inflammatory diseases, characterized by accumulation of activated neutrophils in lesional areas. In the present study, we demonstrate that the human IL-8 Ab HuMab 10F8, which efficiently neutralizes biological activity of this chemokine, reduces the clinical disease activity in patients with PPP. This supports a central role for IL-8 in the pathophysiology of PPP. Our study indicates the feasibility of an immunotherapeutic approach and provides in vivo proof of concept for the application of an anti-human IL-8 Ab for treatment of inflammatory diseases.

HuMab 10F8 was shown to bind rhIL-8 with picomolar affinity and bound both predominant forms of IL-8 expressed in humans: the 77 aa endothelial cell-derived form and the 72 aa monocyte form (32). The effective inhibition of IL-8 binding to human neutrophils, which express CXCR1 and CXCR2 at similar levels, indicated HuMab 10F8 to inhibit IL-8 binding to both receptors. The HuMab 10F8 epitope was found to be discontinuous, and it is formed by three regions within the N-terminal loop and the first and third β-sheet of IL-8. The epitope overlaps with the CXCR1 (and presumably also the CXCR2) docking site for IL-8 (33). The epitope mapping results suggest that, consistent with the efficient inhibition of binding of IL-8 to cells by HuMab 10F8, IL-8 cannot bind HuMab 10F8 and receptor simultaneously. This should be favorable for clinical application of HuMab 10F8, as the Ab therefore cannot induce Fc-mediated immune effector functions (such as complement- and cell-mediated cytotoxicity), which are often suggested to play a role in mediating side-effects. In conclusion, HuMab 10F8 represents an effective blocker of IL-8 activity in which efficient IL-8 neutralization through blockade of ligand-receptor interaction is identified as an important mechanism of action.

Previously, the efficacy of murine IL-8 Ab in acute inflammatory diseases has been demonstrated in a number of animal models, suggesting Ab-mediated neutralization of IL-8 can potentially be used for various human inflammatory disorders (21, 23, 24, 34–38). Few studies have been performed in chronic inflammatory diseases. The anti-IL-8 activity of another human IL-8 mAb, ABX-IL-8 (IgG2/κ), was demonstrated in vitro and in animal models in vivo (30). The result of a placebo-controlled phase IIb clinical trial for treatment of moderate-to-severe psoriasis with this Ab, however, was disappointing (39). This failure might well have resulted from the low and infrequent dosing used in these studies, leading to insufficient Ab concentrations in situ. Additionally, heterogeneity in clearance rates of the human IgG2 Ab resulting from a polymorphism for FcγRIIa that is known to affect IgG2 serum concentrations (40) may have played a role.

Most chronic inflammatory diseases such as psoriasis have multifactorial causes (reviewed in Ref. (41)), which potentially complicate treatment by targeting a single disease-related factor. For psoriasis in particular, the presence of other CXC chemokines with redundant activities, such as MIG (42) and Gro-α (43), may further compromise the success of solely targeting IL-8. However, single Ab treatments can be highly effective when targeting a critical and essential pathway in chronic inflammation, as shown by the success of anti-TNF-α treatments in inflammatory diseases, including refractory psoriaris (44).

We focused on an inflammatory disorder with a strong neutrophil involvement implying an essential role for IL-8 in the pathophysiology for establishment of an in vivo proof of concept for the therapeutic potential of IL-8 targeting. In PPP, accumulation of activated neutrophils and elevated levels of IL-8 in lesional areas are prominent (19, 20, 45). We herein confirm increased production of IL-8, as well as the closely related CXC chemokine Gro-α, to be typical for PPP compared with a number of other cytokines and chemokines (such as MIG and IL-6), which are also elevated in eczema, and TNF-α, being only moderately elevated in PPP. Very high IL-8 levels were detected in washing fluids of PPP lesional areas, compared with those from patients with eczema. Indeed, eczema is described as an inflammatory disease lacking strong neutrophil involvement (46).

Targeting IL-8 in PPP, through treatment with HuMab 10F8, demonstrated strongly reduced disease activity in five different

clinical efficacy endpoints: numbers of fresh pustules, clinical response (≥50% reduction in numbers of fresh pustules), PPP composite severity index, Physician's Global Assessment, and Patient's Symptom Assessment. The reduction in disease activity was mainly observed following multiple dose administration, and to a lesser extent also upon single dose administration. The effects were most pronounced in groups treated with high doses of Ab, yet were also apparent at lower doses. These effects, however, were not unexpected, as the mean C_{max} of the lowest dose achieved was 10 times higher than the IC_{50} for chemotaxis in vitro (IC_{50} of 0.3 μg/ml).

PPP treatment with HuMab 10F8 resulted in dose-dependent decreases in IL-8 concentrations in washing fluids. Notably, the Ab was readily detected in situ in samples obtained during mAb infusion. A priori, we had not anticipated such a rapid passage of mAb from the circulation through the skin into PPP lesions, which represent the actual site of action for IL-8. The in situ neutralization of IL-8 was confirmed by the clinical efficacy of HuMab 10F8 in PPP patients, which was demonstrated for all efficacy endpoints in this clinical trial. Altogether, these data confirmed that IL-8 plays an essential role in PPP and identified HuMab 10F8 as a candidate for treatment of PPP. The presence of the therapeutic Ab in washing fluids implies that the barrier for larger molecules normally existing in the epidermis is compromised in lesional inflamed skin, and indicates mAb-mediated treatments may also be feasible for other skin inflammatory disorders.

In conclusion, we show IL-8 to play a central role in PPP. Using an IL-8-neutralizing Ab, we demonstrate that targeting a single critical factor in this disease characterized by high IL-8 overexpression leads to clinically relevant reductions in disease activity. This observation bears promise for the treatment of other diseases characterized by IL-8 overexpression.

Acknowledgments

We thank Marleen Voorhorst, Wendy Jansen, and Mischa Houtkamp for technical assistance, Leo Koenderman for guidance and provision of laboratory facilities to conduct neutrophil chemotaxis studies, Jerry Slootstra for peptide-guided epitope mapping, Mohan Srinivasan for affinity measurements, Joost Bakker for graphics, and Sigrid Ruuls for critically reviewing the manuscript. We are grateful to the members of the HuMab 10F8 study group and to Drs. Gregor Jemec (Roskilde, Denmark), Niels Veien (Aalborg, Denmark), and Lars Iversen (Aarhus, Denmark) for contributions to this work.

Disclosures

Frank J. Beurskens, Jessica Teeling, David Satijn, Elmieke P. J. Boot, Paul W. H. I. Parren, and Jan G. J. van de Winkel are employees of Genmab BV. Kim M. Knudsen and Ole Baadsgaard are employees of Genmab A/S. D.H. is an employee of Medarex.

References

1. Harada, A., N. Mukaida, and K. Matsushima. 1996. Interleukin 8 as a novel target for intervention therapy in acute inflammatory diseases. *Mol. Med. Today* 2: 482–489.
2. Yoshimura, T., K. Matsushima, S. Tanaka, E. A. Robinson, E. Appella, J. J. Oppenheim, and E. J. Leonard. 1987. Purification of a human monocyte-derived neutrophil chemotactic factor that has peptide sequence similarity to other host defense cytokines. *Proc. Natl. Acad. Sci. USA* 84: 9233–9237.
3. Matsushima, K., K. Morishita, T. Yoshimura, S. Lavu, Y. Kobayashi, W. Lew, E. Appella, H. F. Kung, E. J. Leonard, and J. J. Oppenheim. 1988. Molecular cloning of a human monocyte-derived neutrophil chemotactic factor (MDNCF) and the induction of MDNCF mRNA by interleukin 1 and tumor necrosis factor. *J. Exp. Med.* 167: 1883–1893.
4. Kownatzki, E., A. Kapp, and S. Uhrich. 1986. Novel neutrophil chemotactic factor derived from human peripheral blood mononuclear leucocytes. *Clin. Exp. Immunol.* 64: 214–222.
5. Walz, A., P. Peveri, H. Aschauer, and M. Baggiolini. 1987. Purification and amino acid sequencing of NAF, a novel neutrophil-activating factor produced by monocytes. *Biochem. Biophys. Res. Commun.* 149: 755–761.
6. Van Damme, J., J. Van Beeumen, G. Opdenakker, and A. Billiau. 1988. A novel, NH2-terminal sequence-characterized human monokine possessing neutrophil chemotactic, skin-reactive, and granulocytosis-promoting activity. *J. Exp. Med.* 167: 1364–1376.
7. Baggiolini, M., B. Dewald, and B. Moser. 1994. Interleukin-8 and related chemotactic cytokines: CXC and CC chemokines. *Adv. Immunol.* 55: 97–179.
8. Wuyts, A., P. Proost, and J. Van Damme. 1998. Interleukin-8 and other CXC chemokines. In *The Cytokine Handbook.* A. W. Thomson, ed. Academic Press, Pittsburgh, pp. 271–311.
9. Moore, B. B., D. A. Arenberg, C. L. Addison, M. P. Keane, P. J. Polverini, and R. M. Strieter. 1998. CXC chemokines mechanism of action in regulating tumor angiogenesis. *Angiogenesis* 2: 123–134.
10. Koch, A. E., P. J. Polverini, S. L. Kunkel, L. A. Harlow, L. A. DiPietro, V. M. Elner, S. G. Elner, and R. M. Strieter. 1992. Interleukin-8 as a macrophage-derived mediator of angiogenesis. *Science* 258: 1798–1801.
11. Samanta, A. K., J. J. Oppenheim, and K. Matsushima. 1990. Interleukin 8 (monocyte-derived neutrophil chemotactic factor) dynamically regulates its own receptor expression on human neutrophils. *J. Biol. Chem.* 265: 183–189.
12. Hillyer, P., E. Mordelet, G. Flynn, and D. Male. 2003. Chemokines, chemokine receptors and adhesion molecules on different human endothelia: discriminating the tissue-specific functions that affect leucocyte migration. *Clin. Exp. Immunol.* 134: 431–441.
13. Seitz, M., B. Dewald, N. Gerber, and M. Baggiolini. 1991. Enhanced production of neutrophil-activating peptide-1/interleukin-8 in rheumatoid arthritis. *J. Clin. Invest.* 87: 463–469.
14. Brennan, F. M., C. O. Zachariae, D. Chantry, C. G. Larsen, M. Turner, R. N. Maini, K. Matsushima, and M. Feldmann. 1990. Detection of interleukin 8 biological activity in synovial fluids from patients with rheumatoid arthritis and production of interleukin 8 mRNA by isolated synovial cells. *Eur. J. Immunol.* 20: 2141–2144.
15. Beaulieu, A. D., and S. R. McColl. 1994. Differential expression of two major cytokines produced by neutrophils, interleukin-8 and the interleukin-1 receptor antagonist, in neutrophils isolated from the synovial fluid and peripheral blood of patients with rheumatoid arthritis. *Arthritis Rheum.* 37: 855–859.
16. Grimm, M. C., S. K. Elsbury, P. Pavli, and W. F. Doe. 1996. Interleukin 8: cells of origin in inflammatory bowel disease. *Gut* 38: 90–98.
17. Wiedow, O., and M. Stander. 1989. Entzundungsfordernde Inhaltsstoffe der psoriatischen Epidermis. *Dt. Derm.* 37: 6–8.
18. Schroder, J. M., H. Gregory, J. Young, and E. Christophers. 1992. Neutrophil-activating proteins in psoriasis. *J. Invest. Dermatol.* 98: 241–247.
19. Anttila, H. S., S. Reitamo, P. Erkko, M. Ceska, B. Moser, and M. Baggiolini. 1992. Interleukin-8 immunoreactivity in the skin of healthy subjects and patients with palmoplantar pustulosis and psoriasis. *J. Invest. Dermatol.* 98: 96–101.
20. Ozawa, M., T. Terui, and H. Tagami. 2005. Localization of IL-8 and complement components in lesional skin of psoriasis vulgaris and pustulosis palmaris et plantaris. *Dermatology* 211: 249–255.
21. Sekido, N., N. Mukaida, A. Harada, I. Nakanishi, Y. Watanabe, and K. Matsushima. 1993. Prevention of lung reperfusion injury in rabbits by a monoclonal antibody against interleukin-8. *Nature* 365: 654–657.
22. Harada, A., N. Sekido, T. Akahoshi, T. Wada, N. Mukaida, and K. Matsushima. 1994. Essential involvement of interleukin-8 (IL-8) in acute inflammation. *J. Leukocyte Biol.* 56: 559–564.
23. Broaddus, V. C., A. M. Boylan, J. M. Hoeffel, K. J. Kim, M. Sadick, A. Chuntharapai, and C. A. Hebert. 1994. Neutralization of IL-8 inhibits neutrophil influx in a rabbit model of endotoxin-induced pleurisy. *J. Immunol.* 152: 2960–2967.
24. Wada, T., N. Tomosugi, T. Naito, H. Yokoyama, K. Kobayashi, A. Harada, N. Mukaida, and K. Matsushima. 1994. Prevention of proteinuria by the administration of anti-interleukin 8 antibody in experimental acute immune complex-induced glomerulonephritis. *J. Exp. Med.* 180: 1135–1140.
25. Rosen, K. 1988. Pustulosis palmoplantaris and chronic eczematous hand dermatitis: treatment, epidermal Langerhans cells and association with thyroid disease. *Acta Derm. Venereol. Suppl.* 137: 1–52.
26. Reitamo, S., P. Erkko, A. Remitz, A. I. Lauerma, O. Montonen, and K. Harjula. 1993. Cyclosporine in the treatment of palmoplantar pustulosis. A randomized, double-blind, placebo-controlled study. *Arch. Dermatol.* 129: 1273–1279.
27. Kohler, G., and C. Milstein. 1975. Continuous cultures of fused cells secreting antibody of predefined specificity. *Nature* 256: 495–497.
28. Slootstra, J. W., W. C. Puijk, G. J. Ligtvoet, J. P. Langeveld, and R. H. Meloen. 1996. Structural aspects of antibody-antigen interaction revealed through small random peptide libraries. *Mol. Divers.* 1: 87–96.
29. Timmerman, P., J. Beld, W. C. Puijk, and R. H. Meloen. 2005. Rapid and quantitative cyclization of multiple peptide loops onto synthetic scaffolds for structural mimicry of protein surfaces. *Chembiochem* 6: 821–824.
30. Yang, X. D., J. R. Corvalan, P. Wang, C. M. Roy, and C. G. Davis. 1999. Fully human anti-interleukin-8 monoclonal antibodies: potential therapeutics for the treatment of inflammatory disease states. *J. Leukocyte Biol.* 66: 401–410.
31. Fishwild, D. M., S. L. O'Donnell, T. Bengoechea, D. V. Hudson, F. Harding, S. L. Bernhard, D. Jones, R. M. Kay, K. M. Higgins, S. R. Schramm, and N. Lonberg. 1996. High-avidity human IgGκ monoclonal antibodies from a novel strain of minilocus transgenic mice. *Nat. Biotechnol.* 14: 845–851.
32. Hebert, C. A., F. W. Luscinskas, J. M. Kiely, E. A. Luis, W. C. Darbonne, G. L. Bennett, C. C. Liu, M. S. Obin, M. A. Gimbrone, Jr., and J. B. Baker. 1990. Endothelial and leukocyte forms of IL-8: conversion by thrombin and interactions with neutrophils. *J. Immunol.* 145: 3033–3040.
33. Skelton, N. J., C. Quan, D. Reilly, and H. Lowman. 1999. Structure of a CXC chemokine-receptor fragment in complex with interleukin-8. *Structure* 7: 157–168.

34. Yokoi, K., N. Mukaida, A. Harada, Y. Watanabe, and K. Matsushima. 1997. Prevention of endotoxemia-induced acute respiratory distress syndrome-like lung injury in rabbits by a monoclonal antibody to IL-8. *Lab. Invest.* 76: 375–384.
35. Matsumoto, T., K. Yokoi, N. Mukaida, A. Harada, J. Yamashita, Y. Watanabe, and K. Matsushima. 1997. Pivotal role of interleukin-8 in the acute respiratory distress syndrome and cerebral reperfusion injury. *J. Leukocyte Biol.* 62: 581–587.
36. Dumont, R. A., B. D. Car, N. N. Voitenok, U. Junker, B. Moser, O. Zak, and T. O'Reilly. 2000. Systemic neutralization of interleukin-8 markedly reduces neutrophilic pleocytosis during experimental lipopolysaccharide-induced meningitis in rabbits. *Infect. Immun.* 68: 5756–5763.
37. Folkesson, H. G., M. A. Matthay, C. A. Hebert, and V. C. Broaddus. 1995. Acid aspiration-induced lung injury in rabbits is mediated by interleukin-8-dependent mechanisms. *J. Clin. Invest.* 96: 107–116.
38. Boyle, E. M., Jr., J. C. Kovacich, C. A. Hebert, T. G. Canty, Jr., E. Chi, E. N. Morgan, T. H. Pohlman, and E. D. Verrier. 1998. Inhibition of interleukin-8 blocks myocardial ischemia-reperfusion injury. *J. Thorac. Cardiovasc. Surg.* 116: 114–121.
39. Yan, L., G. M. Anderson, M. De Witte, and M. T. Nakada. 2006. Therapeutic potential of cytokine and chemokine antagonists in cancer therapy. *Eur. J. Cancer* 42: 793–802.
40. Parren, P. W., P. A. Warmerdam, L. C. Boeije, J. Arts, N. A. Westerdaal, A. Vlug, P. J. Capel, L. A. Aarden, and J. G. van de Winkel. 1992. On the interaction of IgG subclasses with the low affinity FcγRIIa (CD32) on human monocytes, neutrophils, and platelets: analysis of a functional polymorphism to human IgG2. *J. Clin. Invest.* 90: 1537–1546.
41. Krueger, G., and C. N. Ellis. 2005. Psoriasis: recent advances in understanding its pathogenesis and treatment. *J. Am. Acad. Dermatol.* 53: S94–S100.
42. Goebeler, M., A. Toksoy, U. Spandau, E. Engelhardt, E. B. Brocker, and R. Gillitzer. 1998. The C-X-C chemokine Mig is highly expressed in the papillae of psoriatic lesions. *J. Pathol.* 184: 89–95.
43. Kulke, R., I. Todt-Pingel, D. Rademacher, J. Rowert, J. M. Schroder, and E. Christophers. 1996. Co-localized overexpression of GRO-α and IL-8 mRNA is restricted to the suprapapillary layers of psoriatic lesions. *J. Invest. Dermatol.* 106: 526–530.
44. Atzeni, F., P. Sarzi-Puttini, A. Doria, L. Iaccarino, and F. Capsoni. 2005. Potential off-label use of infliximab in autoimmune and non-autoimmune diseases: a review. *Autoimmun. Rev.* 4: 144–152.
45. Eriksson, M. O., E. Hagforsen, I. P. Lundin, and G. Michaelsson. 1998. Palmoplantar pustulosis: a clinical and immunohistological study. *Br. J. Dermatol.* 138: 390–398.
46. Willis, C. M., E. Young, D. R. Brandon, and J. D. Wilkinson. 1986. Immunopathological and ultrastructural findings in human allergic and irritant contact dermatitis. *Br. J. Dermatol.* 115: 305–316.